

Masks and Boxes: Combining the Best of Both Worlds for Multi-Object Tracking

Tomasz Stanczyk

Inria centre at Université Côte d’Azur
2004 Rte des Lucioles, 06902 Valbonne, France
tomasz.stanczyk@inria.fr

Francois Bremond

Inria centre at Université Côte d’Azur
2004 Rte des Lucioles, 06902 Valbonne, France
francois.bremond@inria.fr

Abstract

Multi-object tracking (MOT) involves identifying and consistently tracking objects across video sequences. Traditional tracking-by-detection methods, while effective, often require extensive tuning and lack generalizability. On the other hand, segmentation mask-based methods are more generic but struggle with tracking management, making them unsuitable for MOT. We propose a novel approach, McByte, which incorporates a temporally propagated segmentation mask as a strong association cue within a tracking-by-detection framework. By combining bounding box and mask information, McByte enhances robustness and generalizability without per-sequence tuning. Evaluated on four benchmark datasets - DanceTrack, MOT17, SoccerNet-tracking 2022, and KITTI-tracking - McByte demonstrates performance gain in all cases examined. At the same time, it outperforms existing mask-based methods. Implementation code will be provided upon acceptance.

1. Introduction

Multi-object tracking (MOT) is a computer vision task that involves tracking objects (e.g., people) across video frames while maintaining consistent object IDs. MOT detects objects in each frame and associates them across consecutive frames. Applications include surveillance, automated behavior analysis (e.g., in hospitals), and autonomous driving, making reliable MOT trackers essential.

Tracking-by-detection methods [4, 12, 27, 35, 36, 38] use bounding boxes to detect objects in each frame and associate them with those from previous frames, based on cues like position, appearance, and motion. The resulting matches form “tracklets” over consecutive frames. However, these methods often require extensive hyper-parameter tuning for each dataset or even per single sequence, reducing their generalizability and limiting their application across different datasets.

Segmentation mask-based methods [7, 29] generate masks to cover objects and track them across video frames.

Trained on large datasets, these methods aim to capture the semantics of image patches, making them more generic. However, they are not designed for MOT, lacking robust management for tracking multiple entities and struggling to detect new objects entering the scene. Additionally, they rely entirely on mask predictions for object positioning, which can be problematic when the predictions are noisy or inaccurate.

In this paper, we explore using a temporally propagated segmentation mask as an association cue to assess its effectiveness in MOT. We propose a novel tracking-by-detection method that combines segmentation masks and bounding boxes to improve the association between tracklets and detections. The mask is managed according to the tracklet lifespan, with usage constraints to enhance tracking performance. Since the mask propagation model is trained on a large dataset, it makes the entire tracking process more generic. Unlike existing tracking-by-detection methods, our approach does not require tuning hyperparameters for each video sequence.

We evaluate our incorporation of the mask as an association cue against a baseline tracker, showing clear benefits for MOT in our controlled approach. Our tracker is tested on four MOT datasets, achieving the highest performance from tracking-by-detection algorithms on DanceTrack [33], SoccerNet-tracking 2022 [9], and KITTI-tracking [16] (Pedestrian). On MOT17 [28], we see a small improvement over the baseline. These results highlight the advantages of using segmentation masks, eliminating the need for per-sequence hyper-parameter tuning. Visual examples of our designed tracker utilizing the mask as an association cue improving over the baseline algorithm are presented in Figs. 1 and 2.

Our contribution in this work is summarized as follows:

1. We provide an evaluation of the existing mask-based approaches in the MOT domain, demonstrating their unsuitability (Sec. 4.5).
2. We propose a novel approach adapting a temporally propagated object segmentation mask as a strong and

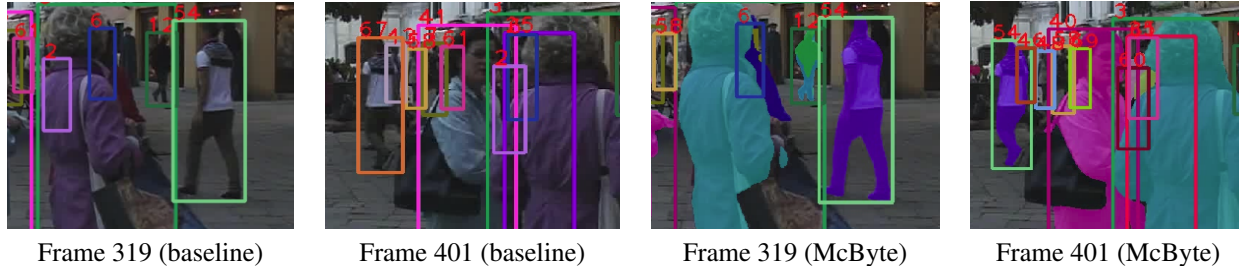


Figure 1. Visual output comparison between the baseline and McByte. With the mask guidance, McByte can handle longer occlusion in the crowd - see the subject with ID 54 on the output of McByte (at frame 319, on the right). Input image data from [28]. Best seen in color.

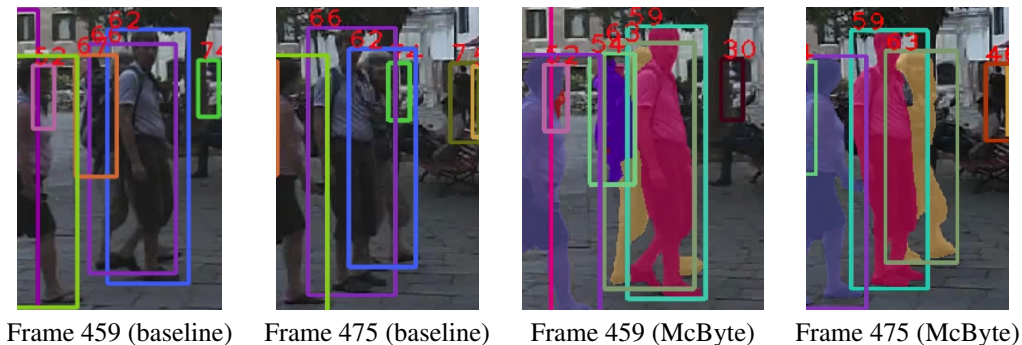


Figure 2. Visual output comparison between the baseline and McByte. With the mask guidance, McByte can handle the association of an ambiguous set of bounding boxes and reduce the identity switches - see the subjects with IDs 59 and 63 on the output of McByte (at frame 459, in the middle). Input image data from [28]. Best seen in color.

powerful cue for MOT, as described in Sec. 3.3.

3. We design an MOT tracking algorithm substantiating the idea and incorporating the mask as an association cue between tracklets and detections, detailed in Secs. 3.1 and 3.2. The tracker overcomes the limitations of mask-based approaches by performing proper tracklet management and including other important association cues as well as the limitations of the baseline tracking-by-detection approaches, by making the tracking process more robust and generic.
4. We evaluate and discuss the use of the mask as an association cue with different conditions within a tracking-by-detection algorithm in the ablation study (Sec. 4.3). Further, we evaluate our tracker incorporating the mask cue on four different datasets (in Sec. 4.4), comparing it to state-of-the-art tracking-by-detection approaches and demonstrating performance gain thanks to the attentive mask usage, while not tuning per-sequence parameters.

2. Related Work

Different types of algorithms tracking multiple objects at the same time have been developed in the community. We

provide a brief overview of the existing methods related to our work.

2.1. Transformer-based methods

Transformer-based methods [13, 14, 37, 39] use attention mechanisms to learn tracking trajectories and object associations from training data, following an end-to-end approach. These methods perform well on video sequences where subjects remain mostly in the scene, such as Dance-Track [33], but struggle with sequences where subjects frequently enter and exit, like in the MOT17 dataset [28], despite being designed for MOT. For this reason, we do not directly compare our method with transformer-based approaches in the main paper, though their results are listed together with the other approaches and ours in the supplementary material, Sec. B.

2.2. Tracking-by-detection methods

The tracking-by-detection approach detects objects in each video frame and associates them into tracklets, linking the same objects across frames.

ByteTrack [38] is a powerful tracking-by-detection algorithm that uses the YOLOX [15] detector, associating tracklets based on the intersection over union (IoU) be-

tween bounding boxes of tracklets and new detections. It provides strong tracklet management and serves as a solid baseline for MOT. Several works have built on ByteTrack. OC-SORT [4] enhances state estimation by computing virtual trajectories during occlusion. StrongSORT [12] adds re-identification (re-ID) features, camera motion compensation, and NSA Kalman filter [11]. C-BIoU [35] extends the association process by buffering (enlarging) bounding boxes, while HybridSORT [36] adds cues like confidence modeling and height-modulated IoU alongside existing strong cues.

Although these algorithms perform well on popular MOT datasets, they are highly sensitive to parameters. ByteTrack, for instance, explicitly tunes parameters like high-confidence detection and tracklet initialization thresholds per test sequence, as noted on its GitHub page¹ and in the code². As we show in the supplementary material, in Sec. D, varying these parameters significantly impacts tracking performance. Extensions of ByteTrack [4, 12, 27, 36], sharing the same code base also rely on per-sequence parameter tuning. This tuning process is costly and impractical for larger datasets like DanceTrack [33], SoccerNet-tracking [9], and KITTI-tracking [16], as well as for generalizing across datasets. In contrast, our method, incorporating the segmentation mask as an association cue, avoids per-sequence tuning, making it more robust and generic, as we further demonstrate in Sec. 4.4.

2.3. Segmentation mask models

Mask creation. The Segment-Anything Model (SAM) [20] is a highly effective image segmentation model trained on a massive dataset, delivering impressive segmentation outputs. Recently, SAM 2 [29] was introduced, enhancing SAM’s performance and enabling video-level segmentation across entire sequences. However, once tracking starts, SAM 2 cannot track new objects, limiting its use in complete MOT tasks. Later in this section, we discuss a SAM 2-based bounding box tracker combined with Grounding Dino [24] (see: *Mask-based tracking systems*).

Mask temporal propagation. XMem [8] is a mask temporal propagation model for video object segmentation, based on the Atkinson-Shiffrin Memory Model [1], enabling long-term tracking of segmentation masks. Its successor, Cutie [6], improves segmentation by incorporating object encoding from mask memory and better distinguishing the object from the background. While useful for re-identifying subjects across frames, both XMem and Cutie are not suitable for MOT as they do not involve bounding

boxes and can provide inaccurate mask predictions as listed in their performance on video object segmentation [6, 8]. Therefore, we propose a novel MOT algorithm that combines temporally propagated masks with bounding boxes, improving tracking performance. Our ablation studies in Sec. 4.3 show that using the mask in a controlled manner, alongside other MOT mechanisms, is more effective than relying solely on the mask signal.

Mask-based tracking systems. Segmentation mask models have already been used to build tracking systems. DEVA [7], which enhances XMem [8], proposes decoupled video segmentation and bi-directional propagation, and builds a tracking system with boxes and masks. However, MOT requires a robust tracklet management and occlusion handling system, which is not available within DEVA.

Grounded SAM 2³ is a tracking system combining Grounding Dino [24] and SAM 2 [29] for video object segmentation, designed to track bounding boxes and maintain object IDs. However, SAM 2’s inability to add new objects once tracking begins makes it unsuitable for MOT. It tracks objects in segments, but merging those segments is not always successful.

MASA [22] is a mask feature-based adapter [3, 18] trained with SAM [20], offering inference modes for video segmentation and object tracking. In tracking, MASA provides features for matching object detections across frames. However, it struggles with longer occlusions and missing or incorrect detections. While MASA has been tested on a few MOT datasets [22], the mentioned limitations weaken its performance and reduce its generalizability across varied datasets.

Existing mask-based tracking algorithms, though trained on large datasets for extracting semantic features, fail to handle challenges like occlusion and track initiation. As shown in Sec. 4.5, their performance on MOT tasks is significantly lower than other methods. Our proposed tracker incorporates the mask as an association cue while leveraging powerful mechanisms like tracklet management and additional cues (e.g., bounding box position, motion). As we demonstrate in Sec. 4.5, our approach performs considerably better than existing mask-based systems, even when they are adapted to MOT format and evaluation.

3. Proposed method

3.1. Preliminaries

Multi-object tracking (MOT) involves tracking detected objects across video frames by forming tracklets that link detections over consecutive frames. In tracking-by-detection methods [4, 12, 27, 35, 36, 38], existing tracklets

¹<https://github.com/ifzhang/ByteTrack>, see: Test on MOT17.

²https://github.com/ifzhang/ByteTrack/blob/main/yolox/evaluators/mot_evaluator.py, lines 146-157 (at the moment of submitting this paper)

³Method not officially published, yet with implementation code available: <https://github.com/IDEA-Research/Grounded-SAM-2>

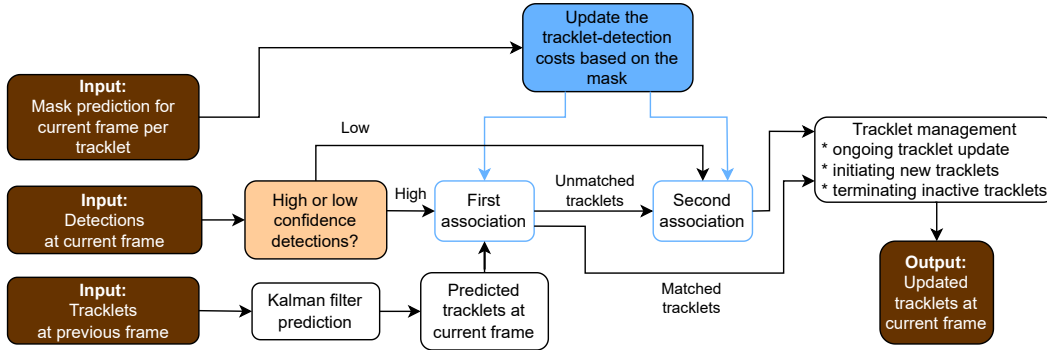


Figure 3. Our tracking pipeline with the mask cue guidance. Mask signal is incorporated as an association cue in the tracklet-detection association steps.

from previous frames are associated with new detections in the current frame. This process uses association cues such as object position and motion to build a cost matrix representing potential tracklet-detection matches. The association problem considered as the bipartite matching problem is then solved using the Hungarian algorithm [21], which matches tracklets with detections to extend them while minimizing total cost. Pairs with costs above the pre-defined matching threshold are excluded.

In our baseline, ByteTrack [38], new detections are split into high and low confidence groups, handled separately in the association process. The baseline uses intersection over union (IoU) as the primary association metric. Tracklet positions are predicted using a Kalman Filter [19] and compared to detection bounding boxes using IoU scores. Cost matrix entries are filled with $1 - \text{IoU}$ for each tracklet-detection pair. Further, tracklet management includes initiating, updating, and terminating tracklets. For more details, we refer the reader to the ByteTrack paper [38].

In our work, we study a temporally propagated segmentation mask as a powerful association cue for MOT. We extend the baseline algorithm [38] and combine the mask information with bounding box information to create our novel **masked-cued** algorithm, which we call McByte. Fig. 3 shows the overview of our tracking pipeline pointing where the mask is involved as an association cue.

In the next sections, we describe the creation and handling of the mask within the tracking algorithm (Sec. 3.2) and our regulated use of the mask as an association cue (Sec. 3.3).

3.2. Mask creation and handling

Since the mask as a cue has to facilitate associating a tracklet with the correct detection, it must be well correlated with the tracklets and handled accordingly. This process is originally not straightforward and thus we design the following approach of mask handling to synchronise it with

the processed tracklets.

During tracking in McByte, each tracklet gets its own mask, which is propagated across frames to update the mask predictions. We use an image segmentation model to create a mask for each new tracklet, which is then passed to a temporal propagator that generates mask predictions for all tracklets during each frame. These predictions are analyzed and used in the tracklet-detection association process, as detailed in Sec. 3.3. We manage the masks in sync with the tracklet management system, creating new masks for new tracklets and removing them when a tracklet is terminated. Visual examples of the masks being used within our tracker are shown in Figs. 1 and 2.

3.3. Regulated use of the mask

A temporally propagated segmentation mask can be a strong association cue if used correctly. However, mask predictions from the temporal propagator can sometimes be incorrect, as seen in related works [6, 8] and thus unreliable, making it essential to regulate the mask’s use as a cue.

In the association process, we update the cost matrix entries using the mask, particularly in cases of ambiguity, where a tracklet could match multiple detections or vice versa. Ambiguity often arises from IoU-based matches when tracked objects are close, causing significant overlap in bounding boxes and similar IoU scores. If IoU is below the matching threshold for more than tracklet-detection pair of a tracklet or of a detection, we treat it as ambiguity.

For each potential ambiguous tracklet-detection match, we apply a strategy consisting of the following conditions.

1. We check if the considered tracklet’s mask is actually visible at the scene. Subjects can be entirely occluded resulting in no mask prediction at the current frame.
2. We check if the mask prediction is confident enough, i.e. if the average mask probability for the given ob-

ject from the mask propagator is above the set mask confidence threshold.

Further, we compute two key ratios between the mask and detection bounding box:

- the bounding box coverage of the mask, referred to as mask match no. 1, mm_1 :

$$mm_1^{i,j} = \frac{|pix(mask(tracklet_i)) \cap pix(bbox_j)|}{|pix(mask(tracklet_i))|} \quad (1)$$

- the mask fill ratio of the bounding box, referred to as mask match no. 2, mm_2 :

$$mm_2^{i,j} = \frac{|pix(mask(tracklet_i)) \cap pix(bbox_j)|}{|pix(bbox_j)|} \quad (2)$$

where $pix(\cdot)$ denotes pixels of the given instance and $mask(\cdot)$ denotes the mask assigned to the tracklet. $|\cdot|$ denotes the cardinality of the set. Note that all $mm_1, mm_2 \in [0, 1]$. In Fig. 4, we show how mm_1 and mm_2 can vary depending on mask and bounding box position. We discuss it more in detail in the supplementary material, Sec. F. Going further with the conditions:

3. We check if the mask fill ratio of the bounding box mm_2 occupies a significant portion of the bounding box.
4. We check if the bounding box coverage of the mask mm_1 is sufficiently high.

Only if all these conditions hold, we update the tracklet-detection association in the cost matrix using the following formula:

$$costs^{i,j} = costs^{i,j} - mm_2^{i,j} \quad (3)$$

where $costs^{i,j}$ denotes the cost between tracklet i and detection j . With this fusion of the available information, we consider both modalities, masks and boxes to enhance the association process. The updated cost matrix, enriched by the mask signal, is passed to the Hungarian matching algorithm to find optimal tracklet-detection pairs.

Following conditions 1-4. ensures that the mask cue is controlled, and the cost matrix is updated only when the mask is reliable. The impact of each condition, along with the absence of any, is demonstrated in the ablation study (Sec. 4.3, Tab. 1). Further details on these conditions are included in the supplementary material, in Sec. F.

Further, using mm_1 directly to influence the cost matrix could be misleading, as multiple masks could fully fit within the same bounding box, all resulting in $mm_1 = 1.0$. Therefore, we use mm_1 only as a gating condition and mm_2 to influence the cost matrix.

Our baseline is optimized for bounding boxes, so we retain the use of the Hungarian matching algorithm over the cost matrix, but we carefully incorporate the mask signal

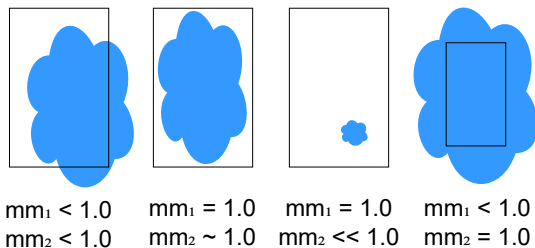


Figure 4. Cases showing the differences in mm_1 and mm_2 (Sec. 3.3) values of a mask (in blue) within a bounding box. The most optimal case for the mask to provide a good guidance is the second one from the left, where both mm_1 and mm_2 are as close to 1 as possible.

to enhance the association process. In the ablation study (Sec. 4.3), we show that combining bounding boxes with the mask is more effective than using the mask alone, and demonstrate the advantages of incorporating the mask signal as an additional association cue over a purely bounding box-based approach.

In Figs. 1 and 2, we show that McByte can handle challenging scenarios such as long-term occlusion in crowd and association of ambiguous boxes due to the mask signal in the controlled manner as an association cue.

3.4. Handling camera motion

When the camera moves, tracklet and detection bounding boxes may become less accurate due to object motion and blurring. To address this, we integrate camera motion compensation (CMC) into our process (which fuses mask and bounding box information) to enhance the accuracy of bounding box estimates. This approach follows existing methods [12, 27]. More details on CMC are provided in the supplementary material, in Sec. F. The final McByte version includes CMC, and its impact is shown in the ablation study in Sec. 4.3, Tab. 1.

4. Experiments and discussion

4.1. Implementation details

For object detections, we use the YOLOX [15] detector pretrained on the relevant dataset, following the practices of our baseline [38], unless stated otherwise. Dataset-specific variations are detailed in the next subsection.

Detections are divided into high and low confidence sets using a threshold of 0.6 for all sequences. For KITTI-tracking (see Sec. 4.2), we adjust the threshold to 0.5 due to different detection quality. In both our baseline and McByte, the new tracklet initialization threshold is set 0.1 higher than the detection confidence threshold. Other parameters match those in the baseline [38].

For mask creation, we use SAM [20], ensuring fair comparison with related works, with the vit_b model and weights from SAM’s authors. As a mask temporal propagator, we use Cutie [6] with the weights provided by the authors, Cutie base mega.

We set the mask confidence threshold (condition 2) to 0.6, mm_2 threshold (condition 3) to 0.05, and mm_1 threshold (condition 4) to 0.9. All experiments are conducted on an Nvidia A100 GPU with 40 GB of memory.

4.2. Datasets and evaluation metrics

We evaluate McByte on four datasets with diverse characteristics: DanceTrack [33], MOT17 [28], SoccerNet-tracking 2022 [9], and KITTI-tracking [16], using different detection sources per dataset as per community practices.

DanceTrack [33] features people performing dances with highly non-linear motion and subtle camera movements, while the number of individuals stays mostly constant. We use YOLOX pre-trained on DanceTrack for detections, following our baseline [38].

MOT17 [28] involves tracking people in public spaces under varying conditions, such as lighting, pedestrian density, and camera stability. YOLOX models, pre-trained by the baseline [38], are used for testing and ablation studies.

SoccerNet-tracking 2022 [9] contains soccer match videos, where players move rapidly and look alike in the same team. Camera movement is always present, and oracle detections (confidence 1.0) are provided by the dataset authors, meaning all detections are treated as high confidence.

KITTI-tracking [16] captures pedestrian and vehicle scenes from a moving car, with varied pedestrian density and frequent camera movement. Following community practices [4, 12], we use PermaTr [34] detections and set a lower confidence threshold of 0.5 due to the different quality of these detections.

We report three standard MOT metrics: HOTA [26], MOTA [2], and IDF1 [31], focusing on HOTA and IDF1 for evaluating tracking performance, as MOTA primarily measures detection accuracy. Higher values in these metrics indicate better performance. Limited number of submissions is allowed on the test set evaluation servers of MOT17 [28] and KITTI-tracking [16].

4.3. Ablation studies

We perform an ablation study to demonstrate the impact of incorporating the mask as an association cue along with the conditions discussed in Sec. 3.3. We evaluate the following variants:

- a1: Uses only the mask signal for association if the mask is visible for the given tracklet, without ambiguity checks (Sec. 3.3). The value of $mm_2^{i,j}$ is directly

Method	HOTA	MOTA	IDF1
baseline [38]: no mask	47.1	88.2	51.9
a1: either mask or no assoc.	48.6	80.8	44.4
a2: either mask or IoU for assoc.	45.3	82.2	41.5
a3: IoU and mask if ambiguity	56.6	89.5	57.0
a4: a3 + mask confidence	57.3	89.6	57.7
a5: a4 + mm_2	58.8	89.6	60.1
a6: a5 + mm_1	62.1	89.7	63.4
McByte: a6 + cmc	62.3	89.8	64.0

Table 1. Ablation study on DanceTrack [33] validation set listing the effects of the imposed constraints on using the mask as an association cue.

Method	HOTA	MOTA	IDF1
Baseline, DanceTrack val	47.1	88.2	51.9
McByte, DanceTrack val	62.3	89.8	64.0
Baseline, SoccerNet-tracking 2022 test	72.1	94.5	75.3
McByte, SoccerNet-tracking 2022 test	85.0	96.8	79.9
Baseline, MOT17 val	68.4	78.2	80.2
McByte, MOT17 val	69.9	78.5	82.8
Baseline, KITTI-tracking test	54.3	63.7	-
McByte, KITTI-tracking test	55.1	66.9	-

Table 2. Ablation study comparing McByte with the baseline [38] on four different datasets.

assigned to $costs^{i,j}$ in Eq. (3). No association occurs if there is no mask.

- a2: Similar to a1, but if the mask is unavailable, intersection over union (IoU) scores are used for association, as in the baseline [38].
- a3: Adds an ambiguity check (Sec. 3.3). If the mask is visible, mask and bounding box information are fused as shown in Eq. (3). If no mask is available, IoU scores are used as in the baseline.
- a4: Builds on a3, incorporating the mask confidence check (condition 2 in Sec. 3.3).
- a5: Extends a4 by adding the mm_2 value check from condition 3 in Sec. 3.3.
- a6: Further extends a5 with the mm_1 value check from condition 4 in Sec. 3.3.

The results of each variant are listed Tab. 1. In variant a1, where only the mask signal is used for association, we can see that despite HOTA increase, IDF1 decrease is present with respect to the baseline. It is caused by the fact that the mask use is uncontrolled and chaotic. With mask possibly providing incorrect results, the association cues can

Method	HOTA	MOTA	IDF1
ByteTrack [38]	47.7	89.6	53.9
OC-SORT [4]	55.1	92.2	54.9
Deep OC-SORT [27]	61.3	92.3	61.5
C-BIoU [35] *	45.8	88.4	52.0
StrongSORT++ [12]	55.6	91.1	55.2
Hybrid-SORT [36]	65.7	91.8	67.4
McByte (ours)	67.1	92.9	68.1

Table 3. Comparing McByte with state-of-the-art tracking-by-detection algorithms on DanceTrack test set [33].

Method	HOTA	MOTA	IDF1
With parameter tuning per sequence			
ByteTrack [38]	63.1	80.3	77.3
StrongSORT++ [12]	64.4	79.6	79.5
OC-SORT [4]	63.2	78.0	77.5
Deep OC-SORT [27]	64.9	79.4	80.6
Hybrid-SORT [36]	64.0	79.9	78.7
Without parameter tuning per sequence			
C-BIoU [35] *	62.4	79.5	77.1
McByte (ours)	64.2	80.2	79.4

Table 4. Comparing McByte with state-of-the-art tracking-by-detection algorithms on MOT17 test set [28].

Method	HOTA	MOTA	IDF1
ByteTrack	72.1	94.5	75.3
OC-SORT [4]	82.0	98.3	76.3
C-BIoU [35] *	72.7	95.4	76.4
McByte (ours)	85.0	96.8	79.9

Table 5. Comparing McByte with state-of-the-art tracking-by-detection algorithms on SoccerNet-tracking 2022 test set [9].

Method	HOTA	MOTA	HOTA	MOTA
	Pedestrian		Car	
ByteTrack [38]	54.3	63.7	47.3	34.9
PermaTr [34]	47.4	65.1	78.0	91.3
OC-SORT [4]	54.7	65.1	76.5	90.3
StrongSORT++ [12]	54.5	67.4	77.8	90.4
McByte (ours)	55.1	66.9	79.9	91.1

Table 6. Comparing McByte with state-of-the-art tracking-by-detection algorithms on KITTI-tracking test set [16].

be misleading. If we perform the association either based only on mask or only on IoU (depending on the availability of the mask), as in variant a2, we might face an inconsistency of the cues between tracklets and detections from the same frame as well as over the next frames. This might lead

to performance degradation. However, when we use properly both cues fusing the available information (variant a3), we can observe significant performance gain. We explain it that the algorithm is initially designed to work on bounding boxes while mask is a valuable guiding cue which can enforce existing association mechanisms. When the mask signal is the only cue or not properly fused with the IoU cue, the lower performance might be obtained (as in a1 and a2).

Adding the conditional check based on mask confidence (variant a4) further improves the performance, because sometimes mask might be uncertain or incorrect providing misleading association guidance. Adding the minimal mm_2 value check (variant a5) also provides performance gain, because this check filters out the tracklet masks which could be considered as a noise or tiny parts of people almost entirely occluded. Another performance gain can be observed with the minimal mm_1 value check (variant a6). This check determines if the mask of the tracked person is actually within the bounding box and not too much outside it. Since the detection box might not be perfect, we allow small part of the tracklet mask to be outside the bounding box, but its major part must be within the bounding box, so that the mask can be used for guiding the association between the considered tracklet-detection pair. As it is shown, it further helps. Finally, we add the camera motion compensation (CMC), denoted as McByte in Tab. 1, which also provides some performance gain. Since the camera is moving in some sequences, CMC improves the quality of the estimated bounding boxes.

We compare our McByte tracking algorithm to the baseline [38] across the four datasets, as shown in Tab. 2. Performance improvements are seen in all cases, though the gains vary by dataset due to differing characteristics. For example, DanceTrack [33] features non-linear motion, where the mask signal is particularly helpful in tracking occluded subjects, whereas IoU might struggle. In SoccerNet-tracking 2022 [9], where occlusions are fewer but motion is more abrupt (e.g., players running), the mask aids in successfully capturing players, despite similar outfits among team members.

The performance gain on MOT17 [28] is smaller than on the previous datasets due to crowded scenes and smaller, distant people, making it harder for the mask to capture them accurately. The quality of detections, especially for small or uncertain bounding boxes, makes it difficult for the mask to comply with our conditions (mm_1 and mm_2), which rely on bounding boxes. KITTI-tracking shows a similar trend, with fewer pedestrians but larger, more easily detectable cars. As shown in Tab. 6, better detection quality for cars leads to higher performance gains. Although gains vary by dataset, McByte consistently improves performance (Tab. 2), demonstrating its robustness and general

applicability.

MyByte also performs better than the baseline when the public detections of a different quality are given. Due to the space limits, we show it in the supplementary material, Sec. E.

4.4. Comparison with state of the art tracking-by-detection methods

We compare McByte with state-of-the-art tracking-by-detection algorithms across the test sets of the four datasets. The results, listed in Tabs. 3 to 6, show that McByte achieves the highest HOTA and IDF1 scores on DanceTrack [33] (Tab. 3) and SoccerNet-tracking 2022 [9] (Tab. 5), as well as the highest HOTA scores on KITTI-tracking [16] (Tab. 6).

The KITTI-tracking test server does not provide IDF1 scores and evaluates both pedestrian and car classes. We also test ByteTrack [38] with the same detection set for comparison. ByteTrack performs poorly on the car class because it is designed for tracking people and is optimized for its pre-trained detections. When using PermaTr [34] detections, which include cars, ByteTrack struggles to generalize, leading to lower performance, though it performs comparably on the pedestrian class.

On the MOT17 [28] test set, unlike the baseline [38] and derived methods [4, 12, 27, 36], we do not tune parameters per sequence. With our mask-based association cue, we achieve improvements over the baseline and comparable performance with other methods, despite not tuning parameters. Due to limited evaluations allowed on the MOT17 test server [10], we are unable to evaluate all listed tracking-by-detection methods without sequence-specific tuning.

Additionally, C-BIoU [35] is marked with an asterisk in Tabs. 3 to 5. As no implementation is published, and not all necessary details for reproduction are provided, we reproduce the method based on the available descriptions and report the best results we have obtained. We describe it more in detail in the supplementary material, Sec. C.

4.5. Comparison with other methods using mask

We evaluate existing mask-based tracking methods: DEVA [7], Grounded SAM 2 [24, 29] and MASA [22] on the MOT17 validation set. Each method is tested with its original settings and with YOLOX [15] trained on MOT17 [28] from our baseline [38], as used in McByte. Results in Tab. 7 show that all methods perform significantly worse than McByte.

DEVA [7] lacks a tracklet management system, leading to chaotic tracklet handling, resulting in negative MOTA scores, which occur when errors exceed the number of objects [10]. Adding YOLOX detections worsens the performance by introducing more redundant and noisy tracklets and masks.

Method	HOTA	MOTA	IDF1
DEVA, original settings	31.8	-89.4	31.3
DEVA, with YOLOX	24.7	-239.7	20.4
Grounded SAM 2, original settings	43.4	18.4	47.6
Grounded SAM 2, with YOLOX	47.5	43.0	54.1
MASA, original settings	45.5	36.9	53.6
MASA, with YOLOX	63.5	74.0	73.6
McByte (ours)	69.9	78.5	82.8

Table 7. Comparison with the other tracking methods using segmentation mask: DEVA [7], Grounded SAM 2 [20, 24] and MASA [22] on MOT17 validation set [28].

Grounded SAM 2 [24, 29] struggles with segment-based tracking, where merging segments into full tracklets is unreliable. Though YOLOX detections improve the performance, the results remain unsatisfactory and far below McByte’s performance.

MASA [22] fails to handle longer occlusions and misses many detections in its original setup, yielding low MOT performance. While YOLOX detections improve its results, it still lags behind McByte and even the baseline due to ongoing challenges with occlusions and missed detections.

These results highlight that existing mask-based methods are unsuitable for MOT. In contrast, McByte effectively combines mask association with bounding box processing and tracklet management, making it better suited for MOT tasks.

More results and details on DEVA, Grounded SAM 2, and MASA experiments are available in the supplementary material, Sec. A

5. Conclusion

In this paper, we explore the use of a temporally propagated segmentation mask as an association cue for MOT. We develop a new mechanism that incorporates the mask into a tracking-by-detection approach, combining mask and bounding box information to improve tracking performance. Results from four datasets show the effectiveness of this approach, with our algorithm boosting MOT performance. Additionally, it outperforms other systems that rely primarily on segmentation masks, highlighting that when carefully managed, the mask can serve as a powerful association cue for MOT.

Acknowledgement

This work was granted access to the HPC resources of IDRIS under the allocation 2024-AD011014370 made by GENCI. The work was performed within the 3IA Côte d’Azur funding.

References

- [1] R.C. Atkinson and R.M. Shiffrin. Human memory: A proposed system and its control processes. volume 2 of *Psychology of Learning and Motivation*, pages 89–195. Academic Press, 1968. [3](#)
- [2] Keni Bernardin and Rainer Stiefelhagen. Evaluating multiple object tracking performance: The clear mot metrics. *EURASIP Journal on Image and Video Processing*, 2008, 01 2008. [6](#)
- [3] Deblina Bhattacharjee, Sabine Süsstrunk, and Mathieu Salzmann. Vision transformer adapters for generalizable multi-task learning, 2023. [3](#)
- [4] Jinkun Cao, Jiangmiao Pang, Xinshuo Weng, Rawal Khirrodkar, and Kris Kitani. Observation-centric sort: Rethinking sort for robust multi-object tracking. In *Proceedings of the IEEE/CVF Conference on Computer Vision and Pattern Recognition*, pages 9686–9696, 2023. [1](#), [3](#), [6](#), [7](#), [8](#), [13](#), [15](#)
- [5] Orcun Cetintas, Guillem Brasó, and Laura Leal-Taixé. Unifying short and long-term tracking with graph hierarchies. In *Proceedings of the IEEE/CVF Conference on Computer Vision and Pattern Recognition (CVPR)*, pages 22877–22887, June 2023. [12](#), [13](#)
- [6] Ho Kei Cheng, Seoung Wug Oh, Brian Price, Joon-Young Lee, and Alexander Schwing. Putting the object back into video object segmentation. In *Proceedings of the IEEE/CVF Conference on Computer Vision and Pattern Recognition (CVPR)*, 2024. [3](#), [4](#), [6](#), [16](#)
- [7] Ho Kei Cheng, Seoung Wug Oh, Brian Price, Alexander Schwing, and Joon-Young Lee. Tracking anything with decoupled video segmentation. In *ICCV*, 2023. [1](#), [3](#), [8](#), [11](#), [12](#)
- [8] Ho Kei Cheng and Alexander G. Schwing. XMem: Long-term video object segmentation with an atkinson-shiffrin memory model. In *ECCV*, 2022. [3](#), [4](#), [16](#)
- [9] Anthony Cioppa, Silvio Giancola, Adrien Deliege, Le Kang, Xin Zhou, Zhiyu Cheng, Bernard Ghanem, and Marc Van Droogenbroeck. Soccernet-tracking: Multiple object tracking dataset and benchmark in soccer videos. In *Proceedings of the IEEE/CVF Conference on Computer Vision and Pattern Recognition*, pages 3491–3502, 2022. [1](#), [3](#), [6](#), [7](#), [8](#), [13](#), [15](#)
- [10] Patrick Dendorfer, Aljossa Ossep, Anton Milan, Daniel Cremers, Ian Reid, Stefan Roth, and Laura Leal-Taixé. Motchallenge: A benchmark for single-camera multiple target tracking. *International Journal of Computer Vision*, 129:1–37, 04 2021. [8](#), [11](#), [15](#)
- [11] Yunhao Du, Junfeng Wan, Yanyun Zhao, Binyu Zhang, Zhihang Tong, and Junhao Dong. Giaotracker: A comprehensive framework for mcmot with global information and optimizing strategies in visdrone 2021. In *Proceedings of the IEEE/CVF International Conference on Computer Vision (ICCV) Workshops*, pages 2809–2819, October 2021. [3](#)
- [12] Yunhao Du, Zhicheng Zhao, Yang Song, Yanyun Zhao, Fei Su, Tao Gong, and Hongying Meng. Strongsort: Make deepsort great again. *IEEE Transactions on Multimedia*, 2023. [1](#), [3](#), [5](#), [6](#), [7](#), [8](#), [13](#), [15](#), [17](#)
- [13] Ruopeng Gao and Limin Wang. MeMOTR: Long-term memory-augmented transformer for multi-object tracking. In *Proceedings of the IEEE/CVF International Conference on Computer Vision (ICCV)*, pages 9901–9910, October 2023. [2](#), [13](#)
- [14] Ruopeng Gao, Yijun Zhang, and Limin Wang. Multiple object tracking as id prediction, 2024. [2](#), [13](#)
- [15] Zheng Ge, Songtao Liu, Feng Wang, Zeming Li, and Jian Sun. Yolox: Exceeding yolo series in 2021. *arXiv preprint arXiv:2107.08430*, 2021. [2](#), [5](#), [8](#), [11](#), [15](#), [16](#)
- [16] Andreas Geiger, Philip Lenz, and Raquel Urtasun. Are we ready for autonomous driving? the kitti vision benchmark suite. In *Conference on Computer Vision and Pattern Recognition (CVPR)*, 2012. [1](#), [3](#), [6](#), [7](#), [8](#), [15](#)
- [17] Kaiming He, Xiangyu Zhang, Shaoqing Ren, and Jian Sun. Deep Residual Learning for Image Recognition. In *Proceedings of 2016 IEEE Conference on Computer Vision and Pattern Recognition, CVPR '16*, pages 770–778. IEEE, June 2016. [11](#)
- [18] Neil Houlsby, Andrei Giurgiu, Stanislaw Jastrzebski, Bruna Morrone, Quentin De Laroussilhe, Andrea Gesmundo, Mona Attariyan, and Sylvain Gelly. Parameter-efficient transfer learning for NLP. In Kamalika Chaudhuri and Ruslan Salakhutdinov, editors, *Proceedings of the 36th International Conference on Machine Learning*, volume 97 of *Proceedings of Machine Learning Research*, pages 2790–2799. PMLR, 09–15 Jun 2019. [3](#)
- [19] R. E. Kalman. A New Approach to Linear Filtering and Prediction Problems. *Journal of Basic Engineering*, 82(1):35–45, 03 1960. [4](#), [17](#)
- [20] Alexander Kirillov, Eric Mintun, Nikhila Ravi, Hanzi Mao, Chloe Rolland, Laura Gustafson, Tete Xiao, Spencer Whitehead, Alexander C. Berg, Wan-Yen Lo, Piotr Dollár, and Ross Girshick. Segment anything. *arXiv:2304.02643*, 2023. [3](#), [6](#), [8](#), [12](#)
- [21] H. W. Kuhn. The hungarian method for the assignment problem. *Naval Research Logistics Quarterly*, 2(1-2):83–97, 1955. [4](#), [15](#)
- [22] Siyuan Li, Lei Ke, Martin Danelljan, Luigi Piccinelli, Mattia Segu, Luc Van Gool, and Fisher Yu. Matching anything by segmenting anything. *CVPR*, 2024. [3](#), [8](#), [11](#), [12](#)
- [23] Tsung-Yi Lin, Michael Maire, Serge J. Belongie, Lubomir D. Bourdev, Ross B. Girshick, James Hays, Pietro Perona, Deva Ramanan, Piotr Dollár, and C. Lawrence Zitnick. Microsoft coco: Common objects in context. *CoRR*, abs/1405.0312, 2014. [11](#)
- [24] Shilong Liu, Zhaoyang Zeng, Tianhe Ren, Feng Li, Hao Zhang, Jie Yang, Chunyuan Li, Jianwei Yang, Hang Su, Jun Zhu, et al. Grounding dino: Marrying dino with grounded pre-training for open-set object detection. *arXiv preprint arXiv:2303.05499*, 2023. [3](#), [8](#), [11](#), [12](#)
- [25] Ze Liu, Yutong Lin, Yue Cao, Han Hu, Yixuan Wei, Zheng Zhang, Stephen Lin, and Baining Guo. Swin transformer: Hierarchical vision transformer using shifted windows. In *Proceedings of the IEEE/CVF International Conference on Computer Vision (ICCV)*, 2021. [11](#)
- [26] Jonathon Luiten, Aljosa Osep, Patrick Dendorfer, Philip Torr, Andreas Geiger, Laura Leal-Taixé, and Bastian Leibe.

- Hota: A higher order metric for evaluating multi-object tracking. *International Journal of Computer Vision*, pages 1–31, 2020. 6
- [27] Gerard Maggolino, Adnan Ahmad, Jinkun Cao, and Kris Kitani. Deep oc-sort: Multi-pedestrian tracking by adaptive re-identification. *arXiv preprint arXiv:2302.11813*, 2023. 1, 3, 5, 7, 8, 13, 15, 17
- [28] A. Milan, L. Leal-Taixé, I. Reid, S. Roth, and K. Schindler. MOT16: A benchmark for multi-object tracking. *arXiv:1603.00831 [cs]*, Mar. 2016. arXiv: 1603.00831. 1, 2, 6, 7, 8, 11, 12, 13, 14, 15, 16
- [29] Nikhila Ravi, Valentin Gabeur, Yuan-Ting Hu, Ronghang Hu, Chaitanya Ryali, Tengyu Ma, Haitham Khedr, Roman Rädle, Chloe Rolland, Laura Gustafson, Eric Mintun, Junting Pan, Kalyan Vasudev Alwala, Nicolas Carion, Chaoyuan Wu, Ross Girshick, Piotr Dollár, and Christoph Feichtenhofer. Sam 2: Segment anything in images and videos. *arXiv preprint arXiv:2408.00714*, 2024. 1, 3, 8, 11
- [30] Shaoqing Ren, Kaiming He, Ross B. Girshick, and Jian Sun. Faster r-cnn: Towards real-time object detection with region proposal networks. In Corinna Cortes, Neil D. Lawrence, Daniel D. Lee, Masashi Sugiyama, and Roman Garnett, editors, *NIPS*, pages 91–99, 2015. 15
- [31] Ergys Ristani, Francesco Solera, Roger Zou, Rita Cucchiara, and Carlo Tomasi. Performance measures and a data set for multi-target, multi-camera tracking. In Gang Hua and Hervé Jégou, editors, *Computer Vision – ECCV 2016 Workshops*, pages 17–35, Cham, 2016. Springer International Publishing. 6
- [32] Ethan Rublee, Vincent Rabaud, Kurt Konolige, and Gary Bradski. Orb: an efficient alternative to sift or surf. pages 2564–2571, 11 2011. 17
- [33] Peize Sun, Jinkun Cao, Yi Jiang, Zehuan Yuan, Song Bai, Kris Kitani, and Ping Luo. Dancetrack: Multi-object tracking in uniform appearance and diverse motion. *arXiv preprint arXiv:2111.14690*, 2021. 1, 2, 3, 6, 7, 8, 11, 12, 13, 15
- [34] Pavel Tokmakov, Jie Li, Wolfram Burgard, and Adrien Gaidon. Learning to track with object permanence. In *ICCV*, 2021. 6, 7, 8, 15
- [35] Fan Yang, Shigeyuki Odashima, Shoichi Masui, and Shan Jiang. Hard to track objects with irregular motions and similar appearances? make it easier by buffering the matching space. In *Proceedings of the IEEE/CVF Winter Conference on Applications of Computer Vision (WACV)*, pages 4799–4808, January 2023. 1, 3, 7, 8, 13, 15
- [36] Mingzhan Yang, Guangxin Han, Bin Yan, Wenhua Zhang, Jinqing Qi, Huchuan Lu, and Dong Wang. Hybrid-sort: Weak cues matter for online multi-object tracking. In *Proceedings of the AAAI Conference on Artificial Intelligence*, volume 38, pages 6504–6512, 2024. 1, 3, 7, 8, 13, 15
- [37] Fangao Zeng, Bin Dong, Yuang Zhang, Tiancai Wang, Xiangyu Zhang, and Yichen Wei. Motr: End-to-end multiple-object tracking with transformer. In *European Conference on Computer Vision (ECCV)*, 2022. 2, 13
- [38] Yifu Zhang, Peize Sun, Yi Jiang, Dongdong Yu, Fucheng Weng, Zehuan Yuan, Ping Luo, Wenyu Liu, and Xinggang Wang. Bytetrack: Multi-object tracking by associating every detection box. 2022. 1, 2, 3, 4, 5, 6, 7, 8, 11, 13, 14, 15, 16
- [39] Yuang Zhang, Tiancai Wang, and Xiangyu Zhang. Motrv2: Bootstrapping end-to-end multi-object tracking by pre-trained object detectors. In *Proceedings of the IEEE/CVF Conference on Computer Vision and Pattern Recognition (CVPR)*, pages 22056–22065, June 2023. 2, 13
- [40] Xingyi Zhou, Rohit Girdhar, Armand Joulin, Philipp Krähenbühl, and Ishan Misra. Detecting twenty-thousand classes using image-level supervision. In *ECCV*, 2022. 11

Appendices

This supplementary material contains the following appendices as referred in the main paper:

- **A** More experiments and details with mask-based tracking systems
- **B** State-of-the-art comparison with offline and transformer-based methods
- **C** More details on our C-BIoU implementation and performance
- **D** Parameter tuning and its impacts
- **E** McByte and ByteTrack on public detections
- **F** McByte components more in detail
 - **F.1** Tracklet mask visibility at the scene
 - **F.2** Mask confidence
 - **F.3** Bounding box coverage (mm1) and mask fill ratio (mm2)
 - **F.4** Camera motion compensation

A. More experiments and details with mask-based tracking systems

We evaluate DEVA [7], Grounded SAM 2 [24,29], and MASA [22] on MOT datasets, saving each bounding box output per frame in MOT format [10]. Grounded SAM 2 and MASA provide object IDs, while for DEVA, we use unique, immutable IDs from the propagated masks associated with each bounding box.

We conduct additional experiments to thoroughly explore the performance differences between the mask-based tracking systems and our McByte. These include several variants on the MOT17 [28] validation set, as well as a corresponding table for the DanceTrack [33] validation set, analogous to the one presented in the main paper.

Tab. 8 presents various experimental variants on the MOT17 validation set, where different detectors and parameters are used. The variants marked with ‡ correspond to those discussed in the main paper.

For DEVA, we first run the default settings using the Grounding Dino [24] detector with the "person" prompt and a confidence threshold of 0.35 to accept bounding boxes. Then, we replace it with the YOLOX [15] detector, trained on the MOT17 dataset from our baseline [38]. We test two threshold values, 0.6 and 0.7, which correspond to the high-confidence detection threshold and the new tracklet initialization in our method, respectively (Sec. 4.1 in the main paper).

For Grounded SAM 2 [24,29], we use the "Video Object Tracking with Continuous ID" version as specified on its GitHub page⁴. Initially, we run it with the original settings, using the Grounding Dino [24] detector with the "person" prompt, a confidence detection threshold of 0.25, and a step value of 20. The step value defines how often detections are processed (e.g., every 20th frame) to create mask tracklets, functioning as the segment length (we refer to tracking objects in segments mentioned in the main paper, Sec. 2.3). We then test an analogous variant with a step value of 100.

Next, we integrate YOLOX detector with weights from our baseline [38] and run variants with step values of 20, 100, and 1, using different bounding box allowance thresholds of 0.25, 0.6, and 0.7 (analogous to the DEVA experiments). We also attempt to run a variant with the segment length set to the entire video sequence, but it fails due to excessive GPU memory requirements. Additionally, this setup would only track objects visible in the first frame.

MASA [22] offers several models for inference. We test variants using two different feature backbones: GroundingDINO [24] (GDino) and ResNet-50 [17] (R50). For the GroundingDINO variant, we use the Detic-SwinB detector [25, 40] with the "person" prompt, applying the original detection confidence threshold of 0.2. We also run a similar variant with the YOLOX detector trained on the COCO [23] dataset, as provided by the authors, using a confidence threshold of 0.3 default for this variant.

We also incorporate the YOLOX detector with weights from our baseline [38] and test variants with detection confidence thresholds of 0.3, 0.6, and 0.7, analogously to DEVA and Grounded SAM 2. Additionally, we run the ResNet-50 feature variants with the YOLOX COCO model (threshold 0.3) and the baseline-pre-trained weights (thresholds 0.3, 0.6, 0.7).

As shown in Tab. 8, McByte outperforms the referenced mask-based systems, making it more suitable for MOT.

Tab. 9 presents the performance of DEVA, Grounded SAM 2, and MASA on the DanceTrack [33] validation set. The listed variants correspond to those marked with ‡ in Tab. 8 and are the ones reported in the main paper.

On DanceTrack, McByte also demonstrates significantly higher performance, reinforcing its effectiveness and suitability for MOT.

B. State-of-the-art comparison with offline and transformer-based methods

There are MOT methods outside the tracking-by-detection domain that perform better than ours on some benchmarks, but usually they are not directly comparable, because they make certain hypotheses, e.g. global optimiza-

⁴<https://github.com/IDEA-Research/Grounded-SAM-2>

Details	HOTA	MOTA	IDF1
DEVA			
GDino "person", th. 0.35 ‡	31.8	-89.4	31.3
YOLOX ByteTrack, th. 0.6 ‡	24.7	-239.7	20.4
YOLOX ByteTrack, th. 0.7	27.0	-187.8	23.7
Grounded SAM 2			
GDino "person", th. 0.25, step 20 ‡	43.4	18.4	47.6
GDino "person", th. 0.25, step 100	44.0	15.5	49.0
YOLOX ByteTrack, th. 0.25, step 20	46.4	36.0	51.6
YOLOX ByteTrack, th. 0.6, step 20 ‡	47.5	43.0	54.1
YOLOX ByteTrack, th. 0.7, step 20	47.4	44.3	54.1
YOLOX ByteTrack, th. 0.25, step 100	46.8	30.2	54.2
YOLOX ByteTrack, th. 0.6, step 100	47.4	34.8	54.9
YOLOX ByteTrack, th. 0.7, step 100	47.4	35.9	54.9
YOLOX ByteTrack, th. 0.25, step 1	43.0	36.2	43.9
YOLOX ByteTrack, th. 0.6, step 1	44.4	44.9	46.5
YOLOX ByteTrack, th. 0.7, step 1	44.3	46.5	46.7
MASA			
GDino feat. Detic-SwinB "person", th 0.2	46.8	24.3	52.1
GDino feat. YOLOX COCO, th 0.3	45.4	36.9	53.1
GDino feat. YOLOX ByteTrack, th 0.3	61.8	71.3	70.8
GDino feat. YOLOX ByteTrack, th 0.6	63.4	73.8	73.3
GDino feat. YOLOX ByteTrack, th 0.7	62.5	72.9	71.9
R50 feat. YOLOX COCO, th 0.3 ‡	45.5	36.9	53.6
R50 feat. YOLOX ByteTrack, th 0.3	62.5	71.5	72.0
R50 feat. YOLOX ByteTrack, th 0.6 ‡	63.5	74.0	73.6
R50 feat. YOLOX ByteTrack, th 0.7	62.6	73.0	72.3
McByte			
McByte (ours)	69.9	78.5	82.8

Table 8. Extended comparison with the other tracking methods using segmentation mask: DEVA [7], Grounded SAM 2 [20, 24] and MASA [22] on MOT17 validation set [28], while changing their parameters. ‡ denotes the variants reported in the main paper and in Tab. 9.

Method	HOTA	MOTA	IDF1
DEVA, original settings	21.9	-347.1	15.8
DEVA, with YOLOX	20.1	-423.9	13.3
Grounded SAM 2, original settings	51.3	73.5	48.0
Grounded SAM 2, with YOLOX	52.9	81.6	49.6
MASA, original settings	38.2	71.9	34.9
MASA, with YOLOX	46.0	85.6	41.1
McByte (ours)	62.3	89.8	64.0

Table 9. Comparison with the other tracking methods using segmentation mask: DEVA [7], Grounded SAM 2 [20, 24] and MASA [22] on DanceTrack validation set [33]. The reported variants correspond to the variants with ‡ symbol in Tab. 8

tion on the whole video. At the same time, these methods perform visibly worse on other benchmarks as we dis-

cuss below. On the contrary, we stress that McByte performs quite well on all the discussed benchmarks (Secs. 4.3 and 4.4 of the main paper). McByte is a tracking-by-detection approach, which is the main focus of our work. For an additional reference, though, we also list performance of the transformer-based and global optimization methods.

Tab. 10 shows extended state-of-the art comparison on MOT17 [28] test set. Transformer-based methods perform visibly lower than the tracking-by-detection methods (including ours) as they struggle with the subjects frequently entering and leaving the scene. In contrast, SUSHI [5], which is a powerful global optimization approach, reaches highly satisfying performance. However, it accesses all the video frames at same time while processing detections and associating the tracklets, which makes it impossible to run in online settings. This makes the performance not directly

Method	HOTA	MOTA	IDF1
Transformer-based			
MOTR [37]	57.8	73.4	68.6
MeMOTR [13]	58.8	72.8	71.5
MOTRv2 [39]	62.0	78.6	75.0
MOTIP [14]	59.2	75.5	71.2
Global optimization			
SUSHI [5]	66.5	81.1	83.1
Tracking-by-detection			
ByteTrack [38]	63.1	80.3	77.3
StrongSORT++ [12]	64.4	79.6	79.5
OC-SORT [4]	63.2	78.0	77.5
Deep OC-SORT [27]	64.9	79.4	80.6
Hybrid-SORT [36]	64.0	79.9	78.7
C-BIoU [35] *	62.4	79.5	77.1
McByte (ours)	64.2	80.2	79.4

Table 10. Extended state-of-the-art method comparison on MOT17 [28] test set.

Method	HOTA	MOTA	IDF1
Transformer-based			
MOTR [37]	54.2	79.7	51.5
MeMOTR [13]	63.4	85.4	65.5
MOTRv2 [39]	73.4	92.1	76.0
MOTIP [14]	67.5	90.3	72.2
Global optimization			
SUSHI [5]	63.3	88.7	63.4
Tracking-by-detection			
ByteTrack [38]	47.7	89.6	53.9
OC-SORT [4]	55.1	92.2	54.9
Deep OC-SORT [27]	61.3	92.3	61.5
C-BIoU [35] *	45.8	88.4	52.0
StrongSORT++ [12]	55.6	91.1	55.2
Hybrid-SORT [36]	65.7	91.8	67.4
McByte (ours)	67.1	92.9	68.1

Table 11. Extended state-of-the-art method comparison on DanceTrack [33] test set.

comparable and therefore, we do not include it in the main paper.

Tab. 11 presents extended state-of-the-art comparison on DanceTrack [33] test set. As in this dataset the subjects remain mostly at the scene, the transformer-based methods performance is more satisfying. The performance of transformer-based methods can be both higher [14, 39] or lower [13, 37] compared to the tracking-by-detection methods. For similar reasons, the global optimization method, SUSHI [5] can also perform higher than the other

tracking-by-detection methods on this dataset, or lower, e.g. when compared to our method. As in the case of the MOT17 benchmark, the performance is not directly comparable and thus not included in the main paper.

C. More details on our C-BIoU implementation and performance

The C-BIoU [35] paper does not provide a public implementation or sufficient details for code reproduction. We implement C-BIoU based on the available information and report the best results on the datasets evaluated by the original algorithm. These results, marked with an asterisk, are shown in the main paper (Tabs. 3 to 5) and in Tabs. 10 and 11 of this supplementary material.

Based on the descriptions in the C-BIoU work [35], especially regarding tracklet management and tracklet-detection association, the core of the method strongly resembles ByteTrack [38]. Thus, we extend ByteTrack by incorporating cascaded buffered intersection over union for the association process. Where C-BIoU does not specify parameters, we default to those used in ByteTrack. For the MOT17 test set, we do not tune detection confidence parameters per sequence (as explained in Sec. 2.2 of the main paper) and apply a fixed 0.6 threshold for all sequences and datasets. Regarding the two buffering scales in C-BIoU, we use the values 0.3 and 0.4, which were reported to result in the best HOTA on the DanceTrack validation set in the C-BIoU paper. Although we also test the values 0.3 and 0.5 (as mentioned in the framework figure from C-BIoU), the 0.3 and 0.4 combination performs slightly better in our experiments.

Additionally, following C-BIoU’s supplementary material, we adopt the most optimal *max_age* values per dataset. The *max_age* parameter defines the maximum lifespan (in frames) of a tracklet that has not been matched to a detection before it is terminated and removed. For DanceTrack [33], we set *max_age* to 100, and for SoccerNet-tracking 2022 [9], we set it to 60. In the case of MOT17 [28], where this value is not directly specified, we test three different *max_age* values: 20, 60, and 100 (as listed in C-BIoU’s supplementary material). We select the value that results in the highest performance on the MOT17 validation set, which is 60, and then use this value for testing on the MOT17 test set to report the final results.

The results are presented in Tabs. 3 to 5 of the main paper. Compared to the baseline, ByteTrack [38], the improvement is modest (Tab. 5) or shows slight degradation (Tabs. 3 and 4). This could be due to tuning issues, as many parameters were not specified in the C-BIoU paper. Specifically, with buffered intersection over union (IoU), the association search space expands, leading to more potential associations and lower IoU-based distances. However, the matching thresholds for the linear association steps (using

Assumed MOT17 [28] sequence correspondence							
MOT17 [28] test sequence	01	03	06	07	08	12	14
ByteTrack [38] thresholds	0.65	0.6	0.65	0.6	0.6	0.7	0.67

Table 12. Different high confidence detection thresholds applied by ByteTrack [38] and most of its successors per test sequences of the MOT17 [28] dataset.

Assumed MOT17 [28] sequence correspondence							
MOT17 test sequence	01	03	06	07	08	12	14
MOT17 train/val sequence	02	04	05	10	09	11	13

Table 13. Our assumed correspondence between training/validation and test sequences of the MOT17 [28] dataset based on the provided descriptions and their characteristics.

HOTA per sequence								
thresholds	overall	02	04	05	09	10	11	13
0.5	67.4	48.6	78.8	61.4	66.6	54.8	62.0	64.4
0.6	68.4	50.8	79.6	61.6	67.6	54.4	63.2	65.5
0.7	68.3	50.7	79.7	58.9	66.4	52.2	66.8	62.0
from ByteTrack [38]	68.0	46.1	79.6	61.1	67.6	54.4	66.8	63.5

Table 14. Ablation study: HOTA comparison of the baseline [38] on the MOT17 [28] validation set per sequence and on all sequences (overall) with varying high confidence detection threshold parameters. The highest scores per column are in bold and marked in red, whereas the lowest scores are in bold and marked in blue.

MOTA per sequence								
thresholds	overall	02	04	05	09	10	11	13
0.5	77.2	54.9	88.7	79.1	86.5	71.2	66.6	74.8
0.6	78.2	58.0	89.0	78.3	86.4	69.6	71.2	77.0
0.7	77.3	58.4	89.9	75.6	84.6	58.7	74.8	73.4
from ByteTrack [38]	78.3	57.1	89.0	78.3	86.3	69.6	74.8	77.0

Table 15. Ablation study: MOTA comparison of the baseline [38] on the MOT17 [28] validation set per sequence and on all sequences (overall) with varying high confidence detection threshold parameters. The highest scores per column are in bold and marked in red, whereas the lowest scores are in bold and marked in blue.

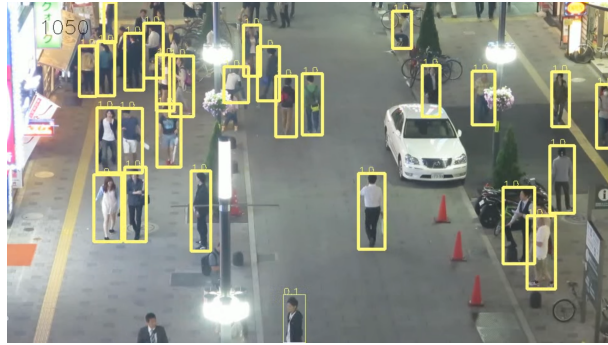
IDF1 per sequence								
thresholds	overall	02	04	05	09	10	11	13
0.5	78.9	58.7	90.7	76.0	78.6	69.2	69.5	83.0
0.6	80.2	61.4	91.6	76.6	79.6	68.5	71.6	84.3
0.7	80.1	60.6	91.7	73.8	78.7	66.7	76.0	79.4
from ByteTrack [38]	79.8	57.1	91.6	76.0	79.6	68.5	76.0	81.7

Table 16. Ablation study: IDF1 comparison of the baseline [38] on the MOT17 [28] validation set per sequence and on all sequences (overall) with varying high confidence detection threshold parameters. The highest scores per column are in bold and marked in red, whereas the lowest scores are in bold and marked in blue.



Private detections

YOLOX model provided by baseline [38]



Public detections

FRCNN model provided by MOT17 [28]

Figure 5. An example of detection quality difference. It can be seen that considerably more bounding boxes are missed in case of public detections, which negatively impacts the MOT performance. Input image data from [28], sequence MOT17-04, last frame (1050). Best seen in color.

the Hungarian Algorithm [21]), which filter out unlikely matches, are not provided. Default thresholds from ByteTrack may allow more matches, introducing unresolved ambiguities and potentially degrading performance.

We do not evaluate C-BIoU on KITTI-tracking test set, because the test evaluation server has a very limited number of submissions per person [16] (less than MOT17 test server [10, 28]). We use these submissions for McByte and our baseline [38]. Besides, the results on KITTI-tracking test set are not reported in the work of C-BIoU [35].

D. Parameter tuning and its impacts

When parameters in tracking-by-detection algorithms [4, 12, 27, 36, 38] are varied, the impact on results can be considerable. We demonstrate this using the MOT17 dataset [28]. Tab. 12 shows different detection confidence threshold values used per MOT17 test sequence by the baseline [38]. Successor methods [4, 12, 27, 36] use the same code base, including these hard-coded parameters (see Sec. 2.2 in the main paper).

We apply both these hard-coded values and a single threshold for all sequences (0.5, 0.6, and 0.7) to ByteTrack [38], evaluating it on the MOT17 validation set. The validation set is made up of the second half of each sequence from the training set. While parameters are typically tuned for the test set in the community, given the test server’s submission limits [10], we match training/validation sequences with their corresponding test sequences. This matching is based on the descriptions and characteristics provided in [28], and we list it in Tab. 13.

Tabs. 14 to 16 present ByteTrack’s performance with these parameter sets for HOTA, MOTA, and IDF1 scores. As demonstrated, even small changes in parameter values can cause noticeable variations in results, both overall and

for individual sequences. We highlight the best scores in red and the lowest in blue.

Tracking results can be highly sensitive to hyperparameters. With parameters tuned per test sequence, tracking-by-detection algorithms [4, 12, 27, 36, 38] achieve high performance, particularly on MOT17. However, tuning parameters per sequence would be laborious and impractical for datasets with many test sequences, like DanceTrack [33] (35 sequences), SoccerNet-tracking 2022 [9] (49 sequences), and KITTI-tracking [16] (29 sequences).

In McByte, we maintain consistent parameters across a dataset, only adjusting them when detection quality differs significantly, i.e., when using PermaTr [34] detections in KITTI-tracking (which still involves using one value for all sequences of a dataset). Despite not having its parameters tuned per sequence, McByte improves upon the baseline [38] and performs comparably to other tracking-by-detection methods that tune parameters for each sequence on the MOT17 dataset [28].

E. McByte and ByteTrack on public detections

We also evaluate McByte and the baseline [38] on the MOT17 [28] validation set using the public detections provided by the dataset authors. The results are shown in Tab. 17, using the FRCNN model variant [30]. There are significant performance differences for both the baseline and McByte when using public detections, which are of lower quality compared to the private YOLOX [15] detections, specifically tuned on MOT17 by the baseline [38]. Public detections tend to miss more objects, leading to many false negatives.

An example comparing the quality of private and public detections is illustrated in Fig. 5. Since tracklets and their masks can only be initiated when a bounding box

Method	HOTA	MOTA	IDF1
MOT17 val, private detections - YOLOX [15] from baseline [38]			
baseline	68.4	78.2	80.2
McByte	69.9	78.5	82.8
MOT17 val, public detections - FRCNN from [28]			
baseline	49.0	44.5	55.3
McByte	50.1	44.6	56.0

Table 17. ByteTrack and McByte with private and public detections on MOT17-val

is detected, McByte’s relative performance gain over the baseline is slightly reduced when using public detections. However, even in this scenario, the mask-based association cue helps resolve ambiguities and improves overall tracking performance, as shown in Tab. 17.

F. McByte components more in detail

In order to ensure reliable use of the mask, we apply several conditions, which we mention in Sec. 3.3 in the main paper. We describe them more in detail in the following subsections.

F.1. Tracklet mask visibility at the scene

In some cases, a tracklet’s mask may not appear in the current frame. This can happen if the subject is completely or mostly occluded, or if the mask temporal propagator fails to predict the mask due to challenges like small visible areas, dense crowds, or poor lighting conditions. When no mask is predicted for a tracklet, its associations with detections are calculated using intersection over union (IoU), as done in the baseline [38].

F.2. Mask confidence

Each predicted pixel in the mask provided by the mask temporal propagator is assigned a confidence probability [6, 8]. To determine if the mask prediction is reliable enough to be used in the tracklet-detection association process, we average these confidence values across all pixels for each tracklet mask separately. If the average confidence falls below our threshold (set to 0.6, as explained in Sec. 4.1 of the main paper), the association relies solely on the intersection over union (IoU) score.

F.3. Bounding box coverage (mm_1) and mask fill ratio (mm_2)

For a more detailed explanation of mm_1 and mm_2 (see Sec. 3.3 in the main paper), we refer to the accompanying figure that illustrates their varying values. For convenience, this figure is also included in the supplementary material, see Fig. 6.

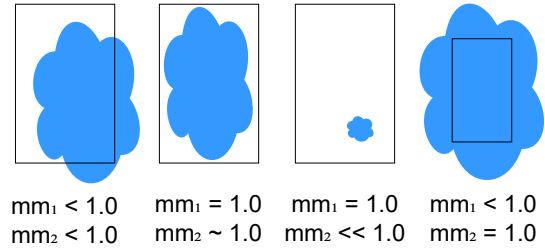


Figure 6. Cases showing the differences in mm_1 and mm_2 (Sec. F.3) values of a mask (in blue) within a bounding box. The most optimal case for the mask to provide a good guidance is the second one from the left, where both mm_1 and mm_2 are as close to 1 as possible.

In the main paper, we define the bounding box coverage of the mask, referred to as mm_1 . It measures the percentage of the tracklet’s mask that falls within the detection’s bounding box for each tracklet-detection pair (if the mask is visible and confident). When the entire mask is within the detection’s bounding box, the mm_1 value is 1.0, as seen in the second and third case from the left in Fig. 6. However, if part of the mask extends outside the bounding box, the mm_1 value decreases, as shown in the first and fourth case from the left in Fig. 6. Bounding boxes can sometimes be slightly inaccurate, so we allow the mm_1 value to be slightly below 1.0, with a threshold of 0.9 (see Sec. 4.1 in the main paper). However, if too much of the mask extends beyond the bounding box, it could indicate that the mask belongs to a different detection, in which case the mask is excluded from influencing the cost of the tracklet-detection match.

In the main paper, we also define the mask fill ratio of the bounding box, referred to as mm_2 . This is calculated for each tracklet-detection pair and measures the percentage of the detection bounding box covered by the mask. If the mask only covers a small portion of the bounding box, the mm_2 value will be low, as illustrated in the third case from the left in Fig. 6. This can indicate a noisy or incorrect mask prediction or that part of another mask is overlapping the bounding box. To avoid misleading associations, we set a minimum threshold for mm_2 (0.05, see Sec. 4.1 in the main paper) to ensure reliable guidance.

For higher coverage, the mm_2 value naturally increases. However, this value alone is not enough to confirm whether the mask tracklet properly matches the detection bounding box. For example, in the first case from the left in Fig. 6, the mask covers most of the bounding box, but it extends significantly beyond it. In the fourth case, mm_2 is 1.0, indicating the mask fully covers the bounding box, but it sticks out even more, making it an unlikely good match. Such situations can occur when one subject is covered by another,

closer to the camera. While mm_2 can approach 1.0, it is rare to see exactly 1.0 in good matches, as subjects (such as people) are not rectangular and do not fully align with their bounding boxes.

For the mask to have the best influence on the tracklet-detection pair match, both mm_1 and mm_2 should be as close to 1.0 as possible, as shown in the second case from the left in Fig. 6.

If both mm_1 and mm_2 meet the required conditions, the cost matrix is updated as described in the main paper (Sec. 3.3):

$$costs^{i,j} = costs^{i,j} - mm_2^{i,j} \quad (4)$$

Since high mm_1 values can be misleading when a mask significantly extends beyond the bounding box, mm_1 is used only as a gating condition to prevent poor matches (e.g., the fourth case from the left in Fig. 6). Instead, we use mm_2 , which better reflects the match quality between a tracklet mask and a detection bounding box, provided mm_1 is sufficiently high.

F.4. Camera motion compensation

For handling camera motion, we use camera motion compensation (CMC), as outlined in Sec. 3.4 of the main paper. Our approach follows the existing methods [12, 27]. Specifically, we compute a warp (transformation) matrix that accounts for camera movement, based on extracted image features, and apply this matrix to the predicted tracklet bounding boxes. This helps adjust for the camera motion, making the tracklet predictions from the Kalman Filter [19] and the associations with detections more accurate, improving the overall tracking performance. For key-point extraction, we use the ORB (Oriented FAST and Rotated BRIEF) approach [32]. For further details, we refer the reader to the related works [12, 27].